JCTC Journal of Chemical Theory and Computation

Article

Cite This: J. Chem. Theory Comput. 2019, 15, 6840−6849

pubs.acs.org/JCTC

Molecular Vibrational Frequencies with Multiple Quantum Protons within the Nuclear-Electronic Orbital Framework

Tanner Culpitt,[†] Yang Yang,[†] Patrick E. Schneider, Fabijan Pavošević, and Sharon Hammes-Schiffer*

Department of Chemistry, Yale University, 225 Prospect Street, New Haven, Connecticut 06520, United States

Supporting Information

ABSTRACT: The nuclear-electronic orbital (NEO) approach treats all electrons and specified nuclei, typically protons, on the same quantum mechanical level. Proton vibrational excitations can be calculated using multicomponent time-dependent density functional theory (NEO-TDDFT) for fixed classical nuclei. Recently the NEO-DFT(V) approach was developed to enable the calculation of molecular vibrational frequencies for modes composed of both classical and quantum nuclei. This approach uses input from NEO-TDDFT to construct an extended NEO Hessian that depends on the expectation values of the quantum protons as well as the classical nuclear coordinates. Herein strategies are devised for extending these approaches to molecules with multiple quantum protons in a self-contained, effective, and computationally practical manner. The NEO-TDDFT method is shown to describe vibrational excitations corresponding to collective nuclear motions, such as linear combinations of proton vibrational excitations. The NEO-DFT(V) approach is shown to incorporate the most significant anharmonic effects in the molecular vibrations, particularly for the hydrogen stretching modes. These theoretical strategies pave the way for a wide range of multicomponent quantum chemistry applications.

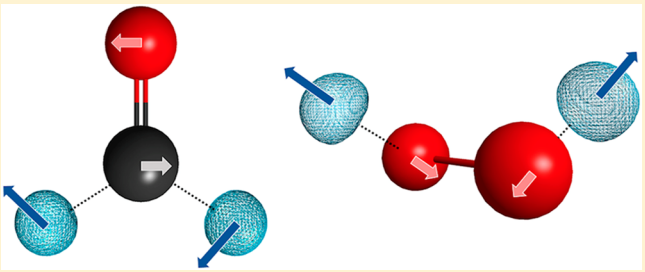

1. INTRODUCTION

To enable the quantum mechanical treatment of more than one type of particle, a variety of multicomponent wave function theory[1−9] and density functional theory (DFT)[10−19] approaches have been developed. The nuclear-electronic orbital (NEO)[3,5−7,9,14,15,17−21] method is a multicomponent quantum chemistry method in which select nuclei, typically protons, are treated quantum mechanically at the same level as the electrons, while at least two other nuclei are treated classically to avoid difficulties with translations and rotations. The Born−Oppenheimer approximation between the electrons and quantum nuclei is avoided in this context, allowing for the simultaneous description of electronic and nuclear quantum effects. Within the NEO framework, NEO-DFT and NEO wave function methods have been demonstrated to accurately describe ground state properties such as proton densities[9,17−19] and proton affinities.[9,18,19] Expanding upon electronic time-dependent density functional theory (TDDFT)[22−27] and equation-of-motion coupled cluster (EOM-CC) theory,[28−31] advances have also been made in calculating vibrational and positronic excitation energies with NEO-TDDFT[20] and NEO-EOM-CCSD,[32] respectively.

Although the NEO approach does not invoke the Born−Oppenheimer separation between the quantum protons and the electrons, it does invoke the Born−Oppenheimer separation between the quantum protons and all classical nuclei. This separation leads to challenges in calculating vibrational frequencies that can be compared to spectroscopic data because the NEO potential energy surface depends on only the coordinates of the classical nuclei, and the quantum protons are assumed to respond instantaneously to the motion of the classical nuclei. As a result, diagonalization of the NEO Hessian matrix produces vibrational modes that depend on only the classical nuclear coordinates without proper coupling to the quantum proton motions. Proton vibrational excitations can be calculated using NEO-TDDFT,[20] but these calculations are performed for fixed classical nuclei, resulting in proton vibrational excitations that are decoupled from the classical nuclei. Recently, the NEO-DFT(V) method was developed to overcome these difficulties and compute full molecular vibrational frequencies.[21]

The NEO-DFT(V) method is capable of calculating vibrational frequencies composed of both the classical and quantum nuclei via diagonalization of an extended NEO Hessian matrix that depends on second derivatives of the NEO energy with respect to the expectation values of the quantum nuclei as well as the coordinates of the classical nuclei. This extended NEO Hessian is constructed with input from NEO-TDDFT, which provides information about the proton vibrational excitations. The effects of zero-point energy and delocalization of the quantum nuclei are included in the geometry optimization, and anharmonic effects are incorporated into the molecular vibrational frequencies dominated by the quantum nuclei. The NEO-DFT(V) method was tested on a set of five molecules and found to produce results

Received: July 4, 2019
Published: October 16, 2019

Downloaded via UNIV OF WISCONSIN-MADISON on February 19, 2020 at 22:50:05 (UTC).
See https://pubs.acs.org/sharingguidelines for options on how to legitimately share published articles.

© 2019 American Chemical Society

DOI: 10.1021/acs.jctc.9b00665
J. Chem. Theory Comput. 2019, 15, 6840−6849

comparable to both experimental data and anharmonic calculations.[21] For all of these test systems, however, only a single proton was treated quantum mechanically. In this paper, we extend the NEO-TDDFT method to molecules with multiple quantum protons, discuss the theoretical challenges associated with performing NEO-DFT(V) calculations with multiple quantum protons, and provide a generalization of the NEO-DFT(V) approach for any number of quantum nuclei.

The manuscript is organized as follows. In Section 2, we review the theory of NEO-DFT(V) and NEO-TDDFT and then explain how properties calculated using NEO-TDDFT can be used to enable practical NEO-DFT(V) calculations with more than one quantum proton. In Section 3, we calculate the vibrational frequencies for a set of four molecules, each with two quantum protons, using NEO-DFT(V). We compare the results to experimental data as well as anharmonic computational results. Section 4 contains concluding remarks.

2. THEORY

2.1. Extended NEO Hessian. For a system with N_c classical nuclei and N_q quantum nuclei, the NEO potential energy surface depends on only the coordinates of the classical nuclei.[3] Because the NEO approach invokes the Born−Oppenheimer separation between the quantum and classical nuclei, the quantum nuclear densities are optimized variationally for a given configuration of the classical nuclei. As a consequence, diagonalization of the $3N_c \times 3N_c$ NEO Hessian matrix provides the harmonic vibrational excitation energies associated with only the classical nuclei. Additionally, these vibrational modes are not properly coupled to the quantum nuclei because the quantum nuclei are assumed to respond instantaneously to any perturbation of the classical nuclei. The strategy of the NEO-DFT(V) method is to compute and diagonalize an extended $3(N_c + N_q) \times 3(N_c + N_q)$ Hessian matrix that includes the proper coupling among all nuclei and produces full molecular vibrational excitation energies that can be compared to spectroscopic data.

The NEO energy can be expressed as

$$E = E(\mathbf{r}_c, \mathbf{r}_q(\mathbf{r}_c)) \tag{1}$$

where $\mathbf{r}_c$ is a $3N_c$-dimensional vector denoting the combined coordinates of the classical nuclei and $\mathbf{r}_q$ is a $3N_q$-dimensional vector denoting the combined expectation values of the quantum nuclei. Specifically, $\mathbf{r}_q$ is a concatenation of $\mathbf{r}_{q_i}$ for each quantum nucleus, and $\mathbf{r}_{q_i}$ is defined as the expectation value of the ith quantum nucleus according to

$$\mathbf{r}_{q_i} = \int \mathbf{r}\rho_{q_i}(\mathbf{r})\, d\mathbf{r} \tag{2}$$

where $\rho_{q_i}(\mathbf{r})$ is the density of the ith quantum nucleus. This approach assumes that each quantum nucleus is spatially localized, rendering them effectively distinguishable. Consequently, each quantum nucleus corresponds to an occupied nuclear orbital that is localized in space, and $\rho_{q_i}(\mathbf{r})$ for a given nucleus is the square of this nuclear orbital. Such an assumption is valid for most molecular systems of interest. From the definition of the NEO energy, which is calculated by variationally optimizing the densities of the electrons and quantum nuclei, the condition

$$\frac{\partial E}{\partial \mathbf{r}_q} = 0 \tag{3}$$

is satisfied for any geometry of the classical nuclei. Specifically, this condition must be satisfied under the constraint that the nuclear determinant used to construct the nuclear density $\rho_q(\mathbf{r})$ minimizes the total NEO energy in eq 1 (see the Supporting Information of ref 21 for details).

As mentioned above, the NEO-DFT(V) method requires the calculation and diagonalization of an extended Hessian that couples the classical and quantum nuclei. This extended Hessian is defined in terms of the $3N_c$ coordinates of the classical nuclei and the $3N_q$ expectation values (i.e., average positions) of the quantum nuclei. Mathematically, the extended Hessian matrix is defined as[21]

$$\mathbf{H}_{NEO}^{ext} = \begin{pmatrix} \mathbf{H}_0 & \mathbf{H}_1^T \\ \mathbf{H}_1 & \mathbf{H}_2 \end{pmatrix} \tag{4}$$

where $\mathbf{H}_0 = \left(\frac{\partial^2 E}{\partial \mathbf{r}_c^2}\right)_{\mathbf{r}_q}$, $\mathbf{H}_1 = \frac{\partial^2 E}{\partial \mathbf{r}_q \partial \mathbf{r}_c}$, and $\mathbf{H}_2 = \left(\frac{\partial^2 E}{\partial \mathbf{r}_q^2}\right)_{\mathbf{r}_c}$. Diagonalization of the mass-weighted form of $\mathbf{H}_{NEO}^{ext}$ provides the full molecular vibrational excitation energies. The remainder of this subsection will outline how each of these submatrices can be calculated.

As a first step toward evaluating these three submatrices, we express the NEO Hessian matrix $\mathbf{H}_{NEO}$ in terms of them. As discussed above, the $3N_c \times 3N_c$ NEO Hessian matrix $\mathbf{H}_{NEO}$ depends on only the classical nuclear coordinates, assuming that the quantum nuclei respond instantaneously to perturbations of the classical nuclei. In practice, this Hessian matrix can be computed analytically or numerically while invoking this Born−Oppenheimer separation between the classical and quantum nuclei.[21] An alternative mathematically rigorous expression for the NEO Hessian matrix $\mathbf{H}_{NEO}$ can be obtained by taking the second derivative of the NEO energy in eq 1 with respect to the classical nuclei:

$$\frac{d^2E}{d\mathbf{r}_c^2} = \left(\frac{\partial^2 E}{\partial \mathbf{r}_c^2}\right)_{\mathbf{r}_q} + 2\frac{\partial^2 E}{\partial \mathbf{r}_c \partial \mathbf{r}_q}\frac{d\mathbf{r}_q}{d\mathbf{r}_c} + \left(\frac{\partial^2 E}{\partial \mathbf{r}_q^2}\right)_{\mathbf{r}_c}\left(\frac{d\mathbf{r}_q}{d\mathbf{r}_c}\right)^2 + \frac{\partial E}{\partial \mathbf{r}_q}\frac{d^2\mathbf{r}_q}{d\mathbf{r}_c^2} \tag{5}$$

This expression can be simplified after some straightforward mathematical manipulations. Differentiating eq 3 with respect to the classical nuclei gives

$$\frac{\partial^2 E}{\partial \mathbf{r}_c \partial \mathbf{r}_q} + \frac{d\mathbf{r}_q}{d\mathbf{r}_c}\left(\frac{\partial^2 E}{\partial \mathbf{r}_q^2}\right)_{\mathbf{r}_c} = 0 \tag{6}$$

and solving for $\frac{d\mathbf{r}_q}{d\mathbf{r}_c}$ yields

$$\frac{d\mathbf{r}_q}{d\mathbf{r}_c} = -\frac{\partial^2 E}{\partial \mathbf{r}_c \partial \mathbf{r}_q}\left(\frac{\partial^2 E}{\partial \mathbf{r}_q^2}\right)_{\mathbf{r}_c}^{-1} \tag{7}$$

Using eqs 3 and 7 allows us to simplify eq 5 as

DOI: 10.1021/acs.jctc.9b00665
J. Chem. Theory Comput. 2019, 15, 6840−6849

$$\frac{d^2E}{d\mathbf{r}_c^2} = \left(\frac{\partial^2 E}{\partial \mathbf{r}_c^2}\right)_{\mathbf{r}_q} - \frac{\partial^2 E}{\partial \mathbf{r}_c \partial \mathbf{r}_q}\left(\frac{\partial^2 E}{\partial \mathbf{r}_q^2}\right)_{\mathbf{r}_c}^{-1}\frac{\partial^2 E}{\partial \mathbf{r}_q \partial \mathbf{r}_c} \tag{8}$$

Finally, eq 8 can be expressed in terms of the submatrices defined above as[21]

$$\mathbf{H}_{NEO} = \mathbf{H}_0 - \mathbf{H}_1^T\mathbf{H}_2^{-1}\mathbf{H}_1 \tag{9}$$

Given this mathematical expression for $\mathbf{H}_{NEO}$, the three submatrices in eq 4 can be computed in a straightforward manner. The $\mathbf{H}_0$ submatrix is the force constant matrix for the classical nuclei with the expectation values of the quantum nuclei fixed, and it is obtained in practice through a rearrangement of eq 9:

$$\mathbf{H}_0 = \mathbf{H}_{NEO} + \mathbf{H}_1^T\mathbf{H}_2^{-1}\mathbf{H}_1 = \mathbf{H}_{NEO} + \mathbf{R}^T\mathbf{H}_2\mathbf{R} \tag{10}$$

Here the $\mathbf{R}$ matrix is defined as

$$\mathbf{R} = \frac{d\mathbf{r}_q}{d\mathbf{r}_c} \tag{11}$$

where

$$\frac{d\mathbf{r}_{q_i}}{d\mathbf{r}_c} = \frac{d}{d\mathbf{r}_c}\int \mathbf{r}\rho_{q_i}(\mathbf{r})\,d\mathbf{r} = \int \mathbf{r}\frac{d\rho_{q_i}(\mathbf{r})}{d\mathbf{r}_c}\,d\mathbf{r} \tag{12}$$

This $\mathbf{R}$ matrix can be calculated analytically or numerically from the gradient of the expectation value of each quantum nucleus with respect to each classical nucleus. From eq 6, it is clear that the $\mathbf{H}_1$ submatrix can be expressed as[21]

$$\mathbf{H}_1 = -\mathbf{H}_2\mathbf{R} \tag{13}$$

Equations 4, 10, and 13 indicate that, if the $\mathbf{H}_2$ matrix is known, then the target $\mathbf{H}_{NEO}^{ext}$ can be constructed and diagonalized. However, $\mathbf{H}_2$ is challenging to compute directly using only information from the nuclear density because it contains second derivatives of the NEO energy with respect to specific components of the combined expectation values $\mathbf{r}_q$ that must vary while other components of $\mathbf{r}_q$ remain fixed.[21] It is therefore desirable to formulate an alternative scheme for constructing $\mathbf{H}_2$.

As defined above, $\mathbf{H}_2$ is the Hessian matrix corresponding to the second derivatives of the energy with respect to the expectation values of the quantum nuclei with the classical nuclei fixed. Within the harmonic oscillator approximation, its associated generalized eigenvalue equation is

$$\mathbf{H}_2\mathbf{U} = \mathbf{M}\mathbf{U}\boldsymbol{\Omega} \tag{14}$$

with the orthonormalization condition

$$\mathbf{U}^\dagger\mathbf{M}\mathbf{U} = \mathbf{I} \tag{15}$$

where $\boldsymbol{\Omega}$ is the diagonal matrix of eigenvalues ω^2, $\mathbf{M}$ is the diagonal mass matrix corresponding to the quantum nuclei, and $\mathbf{U}$ is composed of the eigenvectors, which are denoted normal modes in this context. Typically the Hessian matrix is known and is diagonalized to obtain the normal modes and vibrational frequencies. However, our problem is the reverse in that $\mathbf{H}_2$ needs to be calculated from approximate normal modes and frequencies. For this purpose, eq 14 can be rearranged to be

$$\mathbf{H}_2 = \left(\frac{\partial^2 E}{\partial \mathbf{r}_q^2}\right)_{\mathbf{r}_c} = \mathbf{M}\mathbf{U}\boldsymbol{\Omega}\mathbf{U}^{-1} = \mathbf{M}\mathbf{U}\boldsymbol{\Omega}\mathbf{U}^\dagger\mathbf{M} \tag{16}$$

Thus, $\mathbf{H}_2$ can be constructed if we know the associated eigenvalues ω^2 and eigenvectors $\mathbf{U}$. In our strategy, the quantum proton vibrational frequencies ω used to construct $\boldsymbol{\Omega}$ are approximated by the anharmonic frequencies calculated by NEO-TDDFT. As a result, this approach partially incorporates the anharmonic effects that naturally arise in NEO-TDDFT calculations of vibrational excitations. For single proton systems, the $\mathbf{U}$ matrix was previously constructed from the normal modes associated with the quantum proton as obtained from a conventional electronic Hessian matrix with all nuclei except the proton fixed.[21] While effective, this procedure is not self-contained and adds computational expense. An alternative construction of the $\mathbf{U}$ matrix based on the transition dipole moments obtained from NEO-TDDFT is introduced in the next subsection.

2.2. NEO-TDDFT and the U Matrix Construction. The NEO-DFT method was developed previously for a system composed of electrons and quantum nuclei in a field of fixed classical nuclei. To simplify the discussion, we only consider quantum protons, although the theory is easily extended to other types of quantum nuclei or particles such as positrons. Within the Kohn–Sham formalism, the reference state is defined as the product of electron and proton Slater determinants composed of electronic and protonic orbitals, respectively. The total energy depends on the electron and proton densities, ρ^e and ρ^p, respectively:

$$E[\rho^e, \rho^p] = E_{ext}[\rho^e, \rho^p] + E_{ref}[\rho^e, \rho^p] + E_{exc}[\rho^e] + E_{pxc}[\rho^p] + E_{epc}[\rho^e, \rho^p] \tag{17}$$

Here E denotes the interaction of the electron and proton densities with the external potential due to the fixed classical nuclei, and E_{ref} includes the kinetic energies of the electrons and quantum protons and the classical Coulomb interactions for the reference state. In addition, E_{exc}, E_{pxc}, and E_{epc} denote the electron–electron exchange-correlation functional, the proton–proton exchange-correlation functional, and the electron–proton correlation functional. Application of the variational principle to this total energy functional leads to Kohn–Sham equations for the electrons and quantum protons that are solved iteratively. Our group has developed electron–proton correlation functionals,[19,33] which can be used in conjunction with existing electronic exchange-correlation functionals. Because proton–proton exchange and correlation are negligible for molecular systems associated with localized proton densities, the proton–proton exchange-correlation functional is chosen to be the diagonal Hartree–Fock exchange terms to eliminate self-interaction energy.

The NEO-TDDFT approach was developed to compute electronic and proton vibrational excitations simultaneously in a computationally practical manner. The NEO-TDDFT equations have been derived previously,[20] and only the relevant working equations are presented here. The electronic and protonic excitation energies are calculated by solving

DOI: 10.1021/acs.jctc.9b00665
J. Chem. Theory Comput. 2019, 15, 6840–6849

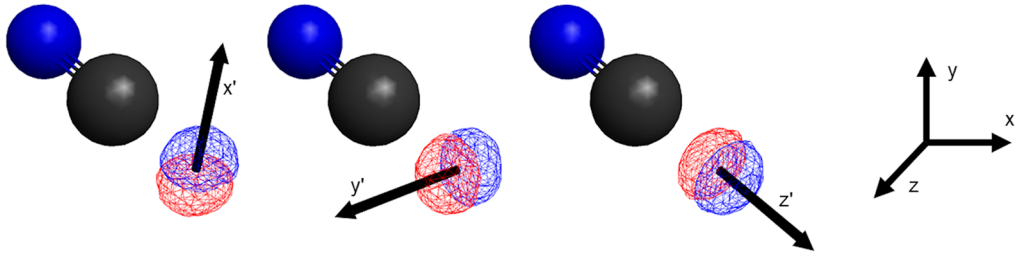

Figure 1. Protonic transition densities and associated transition dipole moment vectors (primed axes) for the three excitations with energies ω_1 (left), ω_2 (center), and ω_3 (right) for HCN. The lab frame coordinate system is depicted as the unprimed coordinate system at the far right of the figure. Each transition dipole moment vector is defined along a primed coordinate axis which is, in general, different than the lab frame.

$$\begin{pmatrix} \mathbf{A}^{e} & \mathbf{B}^{e} & \mathbf{C} & \mathbf{C} \\ \mathbf{B}^{e} & \mathbf{A}^{e} & \mathbf{C} & \mathbf{C} \\ \mathbf{C}^{T} & \mathbf{C}^{T} & \mathbf{A}^{p} & \mathbf{B}^{p} \\ \mathbf{C}^{T} & \mathbf{C}^{T} & \mathbf{B}^{p} & \mathbf{A}^{p} \end{pmatrix} \begin{pmatrix} \mathbf{X}^{e} \\ \mathbf{Y}^{e} \\ \mathbf{X}^{p} \\ \mathbf{Y}^{p} \end{pmatrix} = \omega \begin{pmatrix} \mathbf{I} & 0 & 0 & 0 \\ 0 & -\mathbf{I} & 0 & 0 \\ 0 & 0 & \mathbf{I} & 0 \\ 0 & 0 & 0 & -\mathbf{I} \end{pmatrix} \begin{pmatrix} \mathbf{X}^{e} \\ \mathbf{Y}^{e} \\ \mathbf{X}^{p} \\ \mathbf{Y}^{p} \end{pmatrix} \tag{18}$$

Within the adiabatic approximation, the matrix elements in eq 18 are

$$A^{e}_{ia,jb} = (\varepsilon_a - \varepsilon_i)\delta_{ab}\delta_{ij} + (ia|bj) + \frac{\delta^2 E_{exc}}{\delta P^{e}_{jb}\delta P^{e}_{ai}} + \frac{\delta^2 E_{epc}}{\delta P^{e}_{jb}\delta P^{e}_{ai}} \tag{19}$$

$$B^{e}_{ia,jb} = (ia|jb) + \frac{\delta^2 E_{exc}}{\delta P^{e}_{bj}\delta P^{e}_{ai}} + \frac{\delta^2 E_{epc}}{\delta P^{e}_{bj}\delta P^{e}_{ai}} \tag{20}$$

$$A^{p}_{IA,JB} = (\varepsilon_A - \varepsilon_I)\delta_{AB}\delta_{IJ} + (IA|BJ) + \frac{\delta^2 E_{pxc}}{\delta P^{p}_{JB}\delta P^{p}_{AI}} + \frac{\delta^2 E_{epc}}{\delta P^{p}_{JB}\delta P^{p}_{AI}} \tag{21}$$

$$B^{p}_{IA,JB} = (IA|JB) + \frac{\delta^2 E_{pxc}}{\delta P^{p}_{BJ}\delta P^{p}_{AI}} + \frac{\delta^2 E_{epc}}{\delta P^{p}_{BJ}\delta P^{p}_{AI}} \tag{22}$$

$$C_{ia,JB} = -(ia|BJ) + \frac{\delta^2 E_{epc}}{\delta P^{p}_{JB}\delta P^{e}_{ai}} \tag{23}$$

Here, P denotes the density matrix, ε denotes the orbital energies, and the superscripts e and p denote electrons and protons, respectively. The lower case indices i and j denote occupied electronic orbitals, while the indices a and b denote virtual electronic orbitals. The upper case indices are defined analogously for protonic orbitals. The solution of eq 18 produces the excitation energies ω.

In the current formulation of linear response NEO-TDDFT, only single excitations can be captured, and in principle these excitations could be of electronic, protonic, or mixed electron−proton vibronic character.[20] However, for electronically adiabatic systems, typically the excitations are either electronically or protonically dominated and thus can be described as pure electronic or vibrational excitations to a reasonable approximation. The character of the excitation can be evaluated by examination of the corresponding eigenvector: electronic excitations are dominated by $\mathbf{X}^{e}$, and protonic excitations are dominated by $\mathbf{X}^{p}$. The eigenvectors are subject to the orthonormalization condition[20]

$$\langle X^{e}_{m}|X^{e}_{n}\rangle - \langle Y^{e}_{m}|Y^{e}_{n}\rangle + \langle X^{p}_{m}|X^{p}_{n}\rangle - \langle Y^{p}_{m}|Y^{p}_{n}\rangle = \pm\delta_{mn} \tag{24}$$

In addition to calculating proton vibrational excitation energies, various other quantities can be calculated using information from NEO-TDDFT, such as transition densities, transition dipole moments, and oscillator strengths.[20,34]

In the context of NEO-DFT(V), a quantity that is of particular interest is the transition dipole moment, which is defined for a general NEO excited state $|\Psi_k\rangle$ as

$$\langle\Psi_0|\hat{r}_\gamma|\Psi_k\rangle = \sum_{IA}[X^{p}_{IA}\langle I|r_\gamma|A\rangle + Y^{p}_{IA}\langle A|r_\gamma|I\rangle] + \sum_{ia}[X^{e}_{ia}\langle i|r_\gamma|a\rangle + Y^{e}_{ia}\langle a|r_\gamma|i\rangle] \tag{25}$$

where $\hat{r}_\gamma = \hat{x}$, $\hat{y}$, or $\hat{z}$ for $\gamma = 1$, 2, or 3, respectively, and $\mathbf{X}$ and $\mathbf{Y}$ are obtained from solving eq 18. For notational simplicity, the dependence of the elements of $\mathbf{X}$ and $\mathbf{Y}$ on k in eq 25 is omitted. As mentioned above, the excitations for electronically adiabatic systems can typically be characterized as purely electronic or vibrational. For the molecular vibrational analysis, $|\Psi_k\rangle$ in eq 25 corresponds to the kth proton vibrational excited state, and the terms in the second summation vanish. The resulting transition dipole moment is a vector that reflects the polarization of the protonic transition. The kth transition dipole moment vector can be viewed as the "normal mode" associated with the kth proton vibrational excitation energy ω_k. These vectors are used to construct a rotation matrix $\mathbf{U}$ that in turn can be used in eq 16 for computing the submatrix $\mathbf{H}_2$. This approach provides the rotation matrix $\mathbf{U}$ in an effective, self-contained, and generalizable manner.

As a simple conceptual example, consider the construction of the $\mathbf{H}_2$ matrix for HCN, which has a single quantum proton. To generate $\mathbf{H}_2$, we use NEO-TDDFT to calculate the $3N_p$ proton vibrational excitation energies ω_1, ω_2, and ω_3 that comprise $\mathbf{\Omega}$:

$$\mathbf{\Omega} = \begin{pmatrix} \omega_1^2 & 0 & 0 \\ 0 & \omega_2^2 & 0 \\ 0 & 0 & \omega_3^2 \end{pmatrix} \tag{26}$$

We then use eq 25 to calculate the transition dipole moment vectors associated with each excitation. The transition densities and transition dipole moment vectors associated with the three proton vibrational excitations for HCN are shown in Figure 1.

In Figure 1, the three orthogonal transition dipole moment vectors $|\omega_k\rangle$ associated with the three protonic excitations are represented along axes in a primed coordinate system that may be viewed as the "normal mode" coordinate system for the

DOI: 10.1021/acs.jctc.9b00665
J. Chem. Theory Comput. 2019, 15, 6840−6849

quantum proton. In most cases, the primed coordinate system will not be coincident with the unprimed coordinate system associated with the lab frame, as observed in Figure 1. The vectors $|\omega_k\rangle$ can be represented in the lab frame coordinates using eq 25 according to

$$|\omega_k\rangle = u_x^k|x\rangle + u_y^k|y\rangle + u_z^k|z\rangle \tag{27}$$

where

$$u_\gamma^k = \frac{\langle\Psi_0|\hat{r}_\gamma|\Psi_k\rangle}{\sqrt{m_p \sum_{\gamma=1}^{3} |\langle\Psi_0|\hat{r}_\gamma|\Psi_k\rangle|^2}} \tag{28}$$

Here m_p is the mass of the proton and $u_\gamma^k = u_x^k$, u_y^k, and u_z^k for γ = 1, 2, and 3, respectively. Each $|\omega_k\rangle$ vector forms a column of the transformation matrix $\mathbf{U}$

$$\mathbf{U} = \begin{pmatrix} u_x^1 & u_x^2 & u_x^3 \\ u_y^1 & u_y^2 & u_y^3 \\ u_z^1 & u_z^2 & u_z^3 \end{pmatrix} \tag{29}$$

This matrix corresponds to a transformation or rotation from the normal mode coordinate system to the lab frame coordinate system. Note that this $\mathbf{U}$ matrix satisfies the orthonormalization condition in eq 15.

At this point, we have generated the $\mathbf{U}$ and $\mathbf{\Omega}$ matrices for the case of a single quantum proton and are now equipped to calculate $\mathbf{H}_2$ according to eq 16. In the special case where the "normal mode" coordinate system is coincident with the lab frame coordinate system, the matrix given in eq 29 becomes the $\mathbf{M}^{-1/2}$ matrix, and the $\mathbf{H}_2$ matrix given in eq 16 has the simple diagonal representation

$$\mathbf{H}_2 = \begin{pmatrix} m_p\omega_1^2 & 0 & 0 \\ 0 & m_p\omega_2^2 & 0 \\ 0 & 0 & m_p\omega_3^2 \end{pmatrix} \tag{30}$$

However, this situation is not typical, particularly for nonlinear molecules with multiple protons.

Building on the single proton case, the $\mathbf{U}$ matrix can be constructed for a system with multiple quantum protons. A system of N_p quantum protons will have N_p occupied protonic orbitals that are assumed to be spatially localized. A NEO-TDDFT calculation will yield $3N_p$ protonic excitation energies of interest, where each excitation energy ω will be associated with collective protonic motions. For a given collective mode, we calculate N_p individual transition dipole moment vectors, where each vector is associated with a singly occupied protonic orbital. In the single proton case, each column of the $\mathbf{U}$ matrix was constructed according to eqs 27 and 28. In the multiproton case, a given excitation is now associated with N_p individual transition dipole moment vectors, which may be conceptualized as

$$|\omega_k\rangle \begin{cases} u_x^{k1}|x\rangle + u_y^{k1}|y\rangle + u_z^{k1}|z\rangle\} \rightarrow \text{proton 1} \\ u_x^{k2}|x\rangle + u_y^{k2}|y\rangle + u_z^{k2}|z\rangle\} \rightarrow \text{proton 2} \\ \vdots \\ u_x^{kN_p}|x\rangle + u_y^{kN_p}|y\rangle + u_z^{kN_p}|z\rangle\} \rightarrow \text{proton } N_p \end{cases} \tag{31}$$

For a system composed of N_p quantum protons, the general $3N_p \times 3N_p$ $\mathbf{U}$ matrix used in NEO-DFT(V) is constructed according to

$$\mathbf{U} = \begin{pmatrix} u_x^{11} & u_x^{21} & u_x^{31} & & u_x^{(k-2)1} & u_x^{(k-1)1} & u_x^{k1} \\ u_y^{11} & u_y^{21} & u_y^{31} & \cdots & u_y^{(k-2)1} & u_y^{(k-1)1} & u_y^{k1} \\ u_z^{11} & u_z^{21} & u_z^{31} & & u_z^{(k-2)1} & u_z^{(k-1)1} & u_z^{k1} \\ \vdots & & & \ddots & \vdots & & \\ u_x^{1N_p} & u_x^{2N_p} & u_x^{3N_p} & & u_x^{(k-2)N_p} & u_x^{(k-1)N_p} & u_x^{kN_p} \\ u_y^{1N_p} & u_y^{2N_p} & u_y^{3N_p} & \cdots & u_y^{(k-2)N_p} & u_y^{(k-1)N_p} & u_y^{kN_p} \\ u_z^{1N_p} & u_z^{2N_p} & u_z^{3N_p} & & u_z^{(k-2)N_p} & u_z^{(k-1)N_p} & u_z^{kN_p} \end{pmatrix} \tag{32}$$

where

$$u_\gamma^{kQ} = \frac{\langle\Psi_0|\hat{r}_\gamma^Q|\Psi_k\rangle}{\sqrt{\sum_Q^{N_p} m_Q \sum_{\gamma=1}^{3} |\langle\Psi_0|\hat{r}_\gamma^Q|\Psi_k\rangle|^2}} \tag{33}$$

In eq 33, k is the index specifying a proton vibrational excited state, Q is the index specifying a quantum proton, and m_Q is the mass of the Qth quantum proton (or, more generally, quantum nucleus). For notational clarity in eq 32, $u_\gamma^{kQ} = u_x^{kQ}$, u_y^{kQ}, and u_z^{kQ} for γ = 1, 2, and 3, respectively. The operator $\hat{r}_\gamma^Q$ appearing in eq 33 acts on only the Qth quantum proton, which occupies the Qth nuclear orbital in the ground state, and the corresponding matrix element is defined as

$$\langle\Psi_0|\hat{r}_\gamma^Q|\Psi_k\rangle = \sum_A [X_{QA}^p\langle Q|r_\gamma|A\rangle + Y_{QA}^p\langle A|r_\gamma|Q\rangle] \tag{34}$$

The resulting $\mathbf{U}$ matrix is composed of column vectors, each associated with a specific proton vibrational excited state k. These column vectors are themselves composed of N_p concatenated sets of x, y, z transition dipole moment vector components, where each set is associated with an occupied protonic orbital Q. Note that in the case of a single type of quantum nucleus, the mass m_Q in the expression for u_γ^{kQ} can be factored out in the denominator because it is the same for all quantum nuclei. However, the expression for u_γ^{kQ} in eq 33 is general and is valid for the case of multiple types of quantum nuclei with different masses. This procedure can be used to construct the $\mathbf{U}$ matrix, which in conjunction with the associated $\mathbf{\Omega}$ matrix can be used to compute the $\mathbf{H}_2$ matrix given in eq 16. The $\mathbf{H}_2$ matrix can be used to compute the $\mathbf{H}_0$ and $\mathbf{H}_1$ matrices for the construction of $\mathbf{H}_{NEO}^{ext}$. The eigenvalues and eigenvectors of this extended Hessian provide the molecular vibrational frequencies and normal modes coupling the classical and quantum nuclei.

2.3. Overview of NEO-DFT(V) for Multiple Protons. The overall NEO-DFT(V) procedure described above is well-defined and systematic. Given the reasonable definition of the

DOI: 10.1021/acs.jctc.9b00665
J. Chem. Theory Comput. 2019, 15, 6840−6849

extended Hessian in terms of the classical nuclear coordinates and the expectation values of the quantum nuclei, the expressions for the $\mathbf{H}_0$ and $\mathbf{H}_1$ matrices are mathematically rigorous. The main approximation of this approach lies in the physically motivated construction of the $\mathbf{H}_2$ matrix from the NEO-TDDFT proton vibrational excitation energies and transition dipole moment vectors. A significant advantage of this procedure is that the anharmonicities of the proton vibrational modes are naturally included in the NEO-TDDFT proton vibrational excitation energies used to construct the $\mathbf{H}_2$ matrix. Thus, even though the use of a Hessian to produce vibrational frequencies is based on the harmonic oscillator approximation, the matrix elements of the extended Hessian incorporate the anharmonic effects associated with the quantum protons. As will be shown below, the resulting molecular vibrational frequencies reflect this incorporation of anharmonic effects.

3. RESULTS AND DISCUSSION

We used the NEO-DFT(V) method described above to compute the molecular vibrational frequencies for a set of four molecules, each containing two protons. All molecular geometries were optimized using NEO-DFT with the B3LYP electronic exchange-correlation functional[35,36] and the epc17-2 electron−proton correlation functional,[18] which has been shown to provide accurate proton affinities[18] and accurate NEO-TDDFT excitations.[20,34] The cc-pVDZ electronic basis set[37] was used for the heavy atoms, and the cc-pV5Z electronic basis set[37,38] was used for the quantum protons. An even tempered *6s6p6d6f* nuclear basis set with exponents spanning the range from $4\sqrt{2}$ to 32 was used for the quantum protons. This combination of nuclear and electronic basis sets for the quantum proton has been demonstrated to be effective in calculating accurate proton vibrational excitation energies with the NEO-TDDFT/B3LYP/epc17-2 method.[34] The NEO-DFT(V) and conventional harmonic calculations were performed using a developer version of the GAMESS program.[39] The anharmonic calculations were performed using Gaussian09.[40]

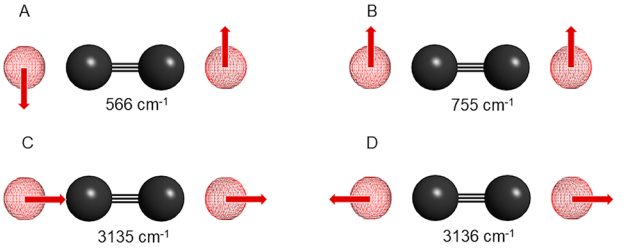

Figure 2. Proton vibrational modes and excitation energies calculated with NEO-TDDFT for HCCH with fixed carbon nuclei. The red mesh indicates the quantum proton density. The molecule is oriented on the *z*-axis with one carbon placed at the origin and a C−C bond distance of 1.207 Å. The expectation values of the quantum protons are −1.086 and 2.293 Å. For each mode, the red arrows indicate the direction of the transition dipole moment vector associated with each quantum proton. Mode (A) is a doubly degenerate CH symmetric bend, mode (B) is a doubly degenerate asymmetric CH bend, mode (C) is an asymmetric CH stretch, and mode (D) is a symmetric CH stretch.

Table 1. U Matrix for HCCH Constructed from the Transition Dipole Moments Computed with NEO-TDDFT[a]

	A	A	B	B	C	D
1*x*	−0.707	0.000	0.707	0.000	0.000	0.000
1*y*	0.000	0.707	0.000	−0.707	0.000	0.000
1*z*	0.000	0.000	0.000	0.000	0.705	−0.710
2*x*	0.707	0.000	0.707	0.000	0.000	0.000
2*y*	0.000	−0.707	0.000	−0.707	0.000	0.000
2*z*	0.000	0.000	0.000	0.000	0.710	0.705

[a]Each column corresponds to a concatenation of transition dipole moment vectors associated with a given NEO-TDDFT vibrational mode, as defined in eqs 32−34. The labels A, B, C, and D correspond to the modes presented in Figure 2. The left-most column indicates the quantum proton (1 or 2) and the Cartesian component (*x*, *y*, or *z*). The slight asymmetry in the *z* components of protons 1 and 2 for columns C and D arises from numerical error and does not impact the NEO-DFT(V) frequencies given in Figure 3. Note that the factor of $m_p^{-1/2}$ has been factored out of the **U** matrix for clarity.

For the ground state NEO-DFT calculations, the nuclear and electronic basis function centers were chosen to be the same for each quantum proton, and the positions of these centers were optimized variationally. For the NEO-TDDFT calculations, the variational ground state positions of the nuclear/electronic basis function centers may not be optimal for calculating accurate proton vibrational excitation energies. The impact of the nuclear/electronic basis function center position on proton vibrational excitation energies calculated with NEO-TDDFT has been investigated in previous work.[34] These previous results indicate that two possible choices for the positions of the nuclear/electronic basis function centers yield accurate and comparable results: (1) the conventional electronic XH bond distance and angle (where X represents an arbitrary heavy atom) and (2) the expectation value of the quantum proton obtained from a ground state NEO-DFT calculation, where the nuclear/electronic basis function centers are optimized variationally.[34] In the present work, the NEO-TDDFT proton vibrational excitation energies used in eq 16 were calculated with the nuclear/electronic basis function centers placed at the expectation values of the quantum protons. This choice has the benefit of being self-contained and therefore more computationally practical, as all information necessary for performing the NEO-TDDFT calculation is obtained from the ground state NEO-DFT calculation.

The procedure for calculating vibrational modes with the NEO-DFT(V) approach is summarized as follows. First, a NEO-DFT geometry optimization is performed on the system of interest. The matrix $\mathbf{H}_{NEO}$ is then calculated numerically by perturbing the classical nuclear coordinates and optimizing the basis function centers for the quantum protons at each perturbed geometry. Using the NEO-DFT optimized geometry for the classical nuclei and the expectation values of the quantum nuclei for the nuclear/electronic basis function center positions, a NEO-TDDFT calculation is performed. The **U** matrix is constructed according to eqs 32 and 33, and this matrix is used in conjunction with the proton vibrational excitation energies to obtain the $\mathbf{H}_2$ matrix given by eq 16. The $\mathbf{H}_2$ matrix is then used together with the **R** matrix to calculate the $\mathbf{H}_0$ and $\mathbf{H}_1$ matrices according to eqs 10 and 13, respectively. Finally, $\mathbf{H}_0$, $\mathbf{H}_1$, and $\mathbf{H}_2$ are used to construct the extended NEO Hessian $\mathbf{H}_{NEO}^{ext}$ in eq 4. Diagonalization of the mass-weighted form of $\mathbf{H}_{NEO}^{ext}$ gives the full molecular vibrational modes.

An important aspect of the NEO-DFT(V) scheme is the use of NEO-TDDFT to compute the proton vibrational excitations

DOI: 10.1021/acs.jctc.9b00665
J. Chem. Theory Comput. 2019, 15, 6840−6849

for fixed classical nuclei. In our previous work,[20,34] the NEO-TDDFT method was applied to molecular systems with only a single quantum proton. Herein, we implement the NEO-TDDFT method for molecular systems with multiple quantum protons. Interestingly, the NEO-TDDFT method produces collective proton vibrational modes that combine motions of multiple quantum nuclei. These collective proton vibrational modes correspond to linear combinations of singly excited determinants and thus are described by linear response NEO-TDDFT. For example, Figure 2 shows the six NEO-TDDFT proton vibrational modes and excitation energies calculated for HCCH with fixed carbon nuclei, where two of the modes are doubly degenerate. Arrows indicating the direction of the transition dipole moment vector associated with each quantum proton are shown for each mode. Table 1 provides the full **U** matrix, which contains the values of all components of the transition dipole moment vectors shown in Figure 2. As mentioned previously, the NEO Hessian depends on only the classical nuclei, assuming the instantaneous response of the quantum nuclei. Thus, the NEO Hessian is one-dimensional in the case of HCCH, with a CC frequency of 2207 cm^{-1}.

The NEO-DFT(V) approach mixes the CC frequency from the NEO Hessian with the NEO-TDDFT modes shown in Figure 2 to produce the coupled molecular vibrational modes shown in Figure 3. Given the three translational and two

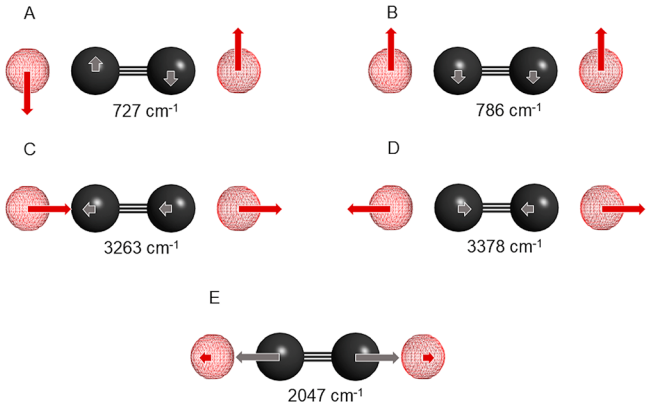

Figure 3. Molecular vibrational modes and excitation energies calculated with NEO-DFT(V) for HCCH. The red mesh indicates the quantum proton density. For each mode, the red and gray arrows indicate the directions of the motions of the quantum protons and carbon atoms, respectively. Mode (A) is a doubly degenerate CH symmetric bend, mode (B) is a doubly degenerate asymmetric CH bend, mode (C) is an asymmetric CH stretch, mode (D) is a symmetric CH stretch, and mode (E) is a symmetric CC stretch.

rotational modes for this linear molecule, this approach provides seven vibrational modes, where two of the distinct modes are doubly degenerate. The NEO-TDDFT proton vibrational excitation energies for the other three molecules studied, namely, H_2O_2, H_2CO, and H_2NF, are provided in the SI. All of these molecules contain only two classical nuclei and therefore correspond to linear geometries in the NEO framework. However, when the quantum nuclei do not maintain this linearity (i.e., the molecule is not linear in a conventional electronic structure calculation), the NEO-DFT(V) approach produces one rotational mode that is associated with a negligible NEO-TDDFT excitation energy. Thus, this approach provides six vibrational modes for the other three molecules.

The NEO-DFT(V) vibrational frequencies for the four molecular systems studied are given in Table 2. Experimental data are provided, along with results obtained from a conventional Hessian calculation within the harmonic oscillator approximation, as well as results obtained from perturbative anharmonic calculations.[41] The average mean unsigned error (MUE) relative to experiment is also reported. Note that the average MUE is virtually the same for the NEO-DFT(V) and the conventional perturbative anharmonic calculations, and both of these methods are more accurate than the conventional harmonic calculations. The errors for specific modes vary, with NEO-DFT(V) typically overestimating bending modes, as well as low energy modes such as the H_2O_2 torsion, to a greater extent than the perturbative anharmonic calculations. Conversely, the conventional perturbative anharmonic calculations typically underestimate the hydrogen stretching modes to a greater extent than do the NEO-DFT(V) calculations, with the largest deviations observed for the asymmetric CH stretch and the NH stretch in H_2CO and H_2NF, respectively. The overall comparability of the NEO-DFT(V) and conventional perturbative anharmonic methods is reasonable because the anharmonicity associated with the hydrogen nuclei is partially incorporated into the NEO-DFT(V) procedure through the NEO-TDDFT proton vibrational excitation energies that are used to construct the $\mathbf{H}_2$ matrix.

4. CONCLUSIONS

In this paper, we have developed and implemented the formalism for treating multiple quantum protons within the NEO-DFT(V) scheme. In this approach, proton vibrational excitation energies and transition dipole moment vectors calculated with NEO-TDDFT are used to construct an extended NEO Hessian matrix, which is defined in terms of the expectation values of the quantum protons as well as the classical nuclear coordinates. Diagonalization of this extended Hessian provides the molecular vibrational frequencies associated with coupled motions of both classical and quantum nuclei. The underlying assumptions of this molecular vibrational analysis are (1) the harmonic approximation inherent to the Hessian framework; (2) the representation of the quantum nuclei by their expectation values; and (3) the use of the NEO-TDDFT proton vibrational excitation energies and transition dipole moment vectors to construct the submatrix associated with the quantum nuclei, thereby partially including the corresponding anharmonicities.

The results indicate that NEO-TDDFT is capable of capturing vibrational excitation energies associated with collective nuclear motion. Moreover, the NEO-DFT(V) calculations for molecules with multiple quantum protons are accurate and comparable to conventional perturbative anharmonic calculations. Anharmonicity is included in NEO-DFT(V) calculations through the NEO-DFT geometry optimizations and the NEO-TDDFT vibrational excitation energies, leading to significantly more accurate hydrogen stretching modes, as well as an overall improvement in accuracy compared to conventional harmonic calculations. The NEO-DFT(V) approach incorporates anharmonicities associated with the quantum nuclei, and the anharmonicities associated with the classical nuclei could be included perturbatively if they are expected to be significant. This formalism lays the foundation for a wide range of applications for multicomponent quantum chemistry methods.

DOI: 10.1021/acs.jctc.9b00665
J. Chem. Theory Comput. 2019, 15, 6840−6849

Table 2. Proton Vibrational Frequencies Calculated with the NEO-DFT(V), Conventional Harmonic, and Conventional Perturbative Anharmonic Methods, as Well as Comparison to Experimental Data[a]

	mode	experiment	NEO-DFT(V)	conv anharmonic	conv harmonic
C_2H_2[b]	symmetric CH bend (2)	612	727	700	569
	aymmetric CH bend (2)	730	786	753	777
	CC stretch	1974	2047	2040	2070
	asymmetric CH stretch	3289	3263	3294	3388
	symmetric CH stretch	3374	3378	3390	3503
H_2O_2[c]	HOOH torsion	254−370	523	248	424
	OO stretch	865−877	957	921	957
	asymmetric OH bend	1265−1274	1314	1249	1332
	symmetric OH bend	1393	1425	1397	1435
	asymmetric OH stretch	3610−3619	3596	3522	3789
	symmetric OH stretch	3609−3618	3599	3528	3792
H_2CO[d]	CH_2 wag	1167	1190	1167	1239
	CH_2 rock	1249	1254	1233	1278
	CH_2 scissor	1500	1477	1484	1567
	CO stretch	1746	1812	1808	1824
	symmetric CH stretch	2783	2724	2706	2882
	asymmetric CH stretch	2843	2772	2651	2935
H_2NF[e]	NF stretch	891	936	910	941
	NH_2 wag	1233	1257	1225	1271
	NH_2 wag	1241	1310	1294	1338
	NH_2 scissor	1564	1556	1550	1638
	symmetric NH stretch	3234	3241	3192	3420
	asymmetric NH stretch	3346	3336	3266	3506
MUE[f]			47	48	92

[a]All frequencies given in cm^{-1}. The average mean unsigned error (MUE) relative to experiment is reported for all methods. All calculations were performed with the B3LYP electronic exchange-correlation functional, and the NEO-DFT(V) excitation energies were computed with the epc17-2 electron−proton correlation functional. The electronic and nuclear basis sets are given in the text. [b]Experimental data from ref 42. [c]Experimental data from ref 43 (HOOH torsion), ref 44 (OO stretch), ref 45 (OH stretches, OH asym. bend), and ref 46 (OH sym. bend). [d]Experimental data from ref 42. [e]Experimental data from ref 47. [f]For H_2O_2 the average of the reported experimental range was used for the calculation of the MUE.

■ ASSOCIATED CONTENT

Supporting Information

The Supporting Information is available free of charge on the ACS Publications website at DOI: 10.1021/acs.jctc.9b00665.

Table of NEO-TDDFT vibrational excitation energies (PDF)

■ AUTHOR INFORMATION

Corresponding Author

*(S.H.-S.) E-mail: sharon.hammes-schiffer@yale.edu.

ORCID

Yang Yang: 0000-0001-8572-5155

Sharon Hammes-Schiffer: 0000-0002-3782-6995

Author Contributions

†(T.C. and Y.Y.) These authors contributed equally to this work.

Notes

The authors declare no competing financial interest.

■ ACKNOWLEDGMENTS

We thank Zhen (Coraline) Tao for helpful discussions. This work was supported by the National Science Foundation Grant No. CHE-1762018. P.E.S. is supported by a National Science Foundation Graduate Research Fellowship Grant No. DGE-1752134.

■ REFERENCES

(1) Thomas, I. L. Protonic Structure of Molecules. I. Ammonia Molecules. *Phys. Rev.* **1969**, *185*, 90−94.

(2) Tachikawa, M.; Mori, K.; Nakai, H.; Iguchi, K. An extension of ab initio molecular orbital theory to nuclear motion. *Chem. Phys. Lett.* **1998**, *290*, 437−442.

(3) Webb, S. P.; Iordanov, T.; Hammes-Schiffer, S. Multiconfigurational nuclear-electronic orbital approach: Incorporation of nuclear quantum effects in electronic structure calculations. *J. Chem. Phys.* **2002**, *117*, 4106−4118.

(4) Nakai, H.; Sodeyama, K. Many-body effects in nonadiabatic molecular theory for simultaneous determination of nuclear and electronic wave functions: Ab initio NOMO/MBPT and CC methods. *J. Chem. Phys.* **2003**, *118*, 1119−1127.

(5) Swalina, C.; Pak, M. V.; Hammes-Schiffer, S. Alternative formulation of many-body perturbation theory for electron-proton correlation. *Chem. Phys. Lett.* **2005**, *404*, 394−399.

(6) Chakraborty, A.; Pak, M. V.; Hammes-Schiffer, S. Inclusion of explicit electron-proton correlation in the nuclear-electronic orbital approach using Gaussian-type geminal functions. *J. Chem. Phys.* **2008**, *129*, 014101.

(7) Sirjoosingh, A.; Pak, M. V.; Swalina, C.; Hammes-Schiffer, S. Reduced explicitly correlated Hartree-Fock approach within the nuclear-electronic orbital framework: Theoretical formulation. *J. Chem. Phys.* **2013**, *139*, 034102.

(8) Bubin, S.; Pavanello, M.; Tung, W.-C.; Sharkey, K. L.; Adamowicz, L. Born-Oppenheimer and Non-Born-Oppenheimer, Atomic and Molecular Calculations with Explicitly Correlated Gaussians. *Chem. Rev.* **2013**, *113*, 36−79.

(9) Pavošević, F.; Culpitt, T.; Hammes-Schiffer, S. Multicomponent Coupled Cluster Singles and Doubles Theory within the Nuclear-

DOI: 10.1021/acs.jctc.9b00665
J. Chem. Theory Comput. 2019, 15, 6840−6849

Electronic Orbital Framework. *J. Chem. Theory Comput.* **2019**, *15*, 338−347.
(10) Capitani, J. F.; Nalewajski, R. F.; Parr, R. G. Non Born-Oppenheimer density functional theory of molecular systems. *J. Chem. Phys.* **1982**, *76*, 568−573.
(11) Gidopoulos, N. Kohn-Sham equations for multicomponent systems: The exchange and correlation energy functional. *Phys. Rev. B: Condens. Matter Mater. Phys.* **1998**, *57*, 2146−2152.
(12) Kreibich, T.; Gross, E. K. U. Multicomponent Density-Functional Theory for Electrons and Nuclei. *Phys. Rev. Lett.* **2001**, *86*, 2984−2987.
(13) Udagawa, T.; Tachikawa, M. H/D isotope effect on porphine and porphycene molecules with multicomponent hybrid density functional theory. *J. Chem. Phys.* **2006**, *125*, 244105.
(14) Pak, M. V.; Chakraborty, A.; Hammes-Schiffer, S. Density Functional Theory Treatment of Electron Correlation in the Nuclear-Electronic Orbital Approach. *J. Phys. Chem. A* **2007**, *111*, 4522−4526.
(15) Chakraborty, A.; Pak, M. V.; Hammes-Schiffer, S. Development of Electron-Proton Density Functionals for Multicomponent Density Functional Theory. *Phys. Rev. Lett.* **2008**, *101*, 153001.
(16) Chakraborty, A.; Pak, M. V.; Hammes-Schiffer, S. Properties of the exact universal functional in multicomponent density functional theory. *J. Chem. Phys.* **2009**, *131*, 124115.
(17) Yang, Y.; Brorsen, K. R.; Culpitt, T.; Pak, M. V.; Hammes-Schiffer, S. Development of a practical multicomponent density functional for electron-proton correlation to produce accurate proton densities. *J. Chem. Phys.* **2017**, *147*, 114113.
(18) Brorsen, K. R.; Yang, Y.; Hammes-Schiffer, S. Multicomponent Density Functional Theory: Impact of Nuclear Quantum Effects on Proton Affinities and Geometries. *J. Phys. Chem. Lett.* **2017**, *8*, 3488−3493.
(19) Brorsen, K. R.; Schneider, P. E.; Hammes-Schiffer, S. Alternative forms and transferability of electron-proton correlation functionals in nuclear-electronic orbital density functional theory. *J. Chem. Phys.* **2018**, *149*, 044110.
(20) Yang, Y.; Culpitt, T.; Hammes-Schiffer, S. Multicomponent Time-Dependent Density Functional Theory: Proton and Electron Excitation Energies. *J. Phys. Chem. Lett.* **2018**, *9*, 1765−1770.
(21) Yang, Y.; Schneider, P. E.; Culpitt, T.; Pavošević, F.; Hammes-Schiffer, S. Molecular Vibrational Frequencies within the Nuclear-Electronic Orbital Framework. *J. Phys. Chem. Lett.* **2019**, *10*, 1167−1172.
(22) Casida, M. E. Time-dependent density functional response theory of molecular systems: theory, computational methods, and functionals. In *Recent Developments and Applications of Modern Density Functional Theory*; Seminario, J., Ed.; Elsevier Science: 1996; Vol. *4*, pp 391−439.
(23) Dreuw, A.; Head-Gordon, M. Single-Reference ab Initio Methods for the Calculation of Excited States of Large Molecules. *Chem. Rev.* **2005**, *105*, 4009−4037.
(24) Burke, K.; Werschnik, J.; Gross, E. K. U. Time-dependent density functional theory: Past, present, and future. *J. Chem. Phys.* **2005**, *123*, 062206.
(25) Ulrich, C. A. *Time-Dependent Density-Functional Theory: Concepts and Applications*; Oxford University Press: Oxford, 2012.
(26) Maitra, N. T. Perspective: Fundamental aspects of time-dependent density functional theory. *J. Chem. Phys.* **2016**, *144*, 220901.
(27) Goings, J. J.; Lestrange, P. J.; Li, X. Real-time time-dependent electronic structure theory. *Wiley Interdisciplinary Reviews: Computational Molecular Science* **2018**, *8*, No. e1341.
(28) Stanton, J. F.; Bartlett, R. J. The equation of motion coupled cluster method. A systematic biorthogonal approach to molecular excitation energies, transition probabilities, and excited state properties. *J. Chem. Phys.* **1993**, *98*, 7029−7039.
(29) Comeau, D. C.; Bartlett, R. J. The equation-of-motion coupled-cluster method. Applications to open- and closed-shell reference states. *Chem. Phys. Lett.* **1993**, *207*, 414−423.
(30) Levchenko, S. V.; Krylov, A. I. Equation-of-motion spin-flip coupled-cluster model with single and double substitutions: Theory and application to cyclobutadiene. *J. Chem. Phys.* **2004**, *120*, 175−185.
(31) Krylov, A. I. Equation-of-Motion Coupled-Cluster Methods for Open-Shell and Electronically Excited Species: The Hitchhiker's Guide to Fock Space. *Annu. Rev. Phys. Chem.* **2008**, *59*, 433−462.
(32) Pavošević, F.; Hammes-Schiffer, S. Multicomponent equation-of-motion coupled cluster singles and doubles: Theory and calculation of excitation energies for positronium hydride. *J. Chem. Phys.* **2019**, *150*, 161102.
(33) Yang, Y.; Brorsen, K. R.; Culpitt, T.; Pak, M. V.; Hammes-Schiffer, S. Development of a practical multicomponent density functional for electron-proton correlation to produce accurate proton densities. *J. Chem. Phys.* **2017**, *147*, 114113.
(34) Culpitt, T.; Yang, Y.; Pavošević, F.; Tao, Z.; Hammes-Schiffer, S. Enhancing the applicability of multicomponent time-dependent density functional theory. *J. Chem. Phys.* **2019**, *150*, 201101.
(35) Lee, C.; Yang, W.; Parr, R. G. Development of the Colle-Salvetti correlation-energy formula into a functional of the electron density. *Phys. Rev. B: Condens. Matter Mater. Phys.* **1988**, *37*, 785−789.
(36) Becke, A. D. Density functional thermochemistry. III. The role of exact exchange. *J. Chem. Phys.* **1993**, *98*, 5648−5652.
(37) Dunning, T. H. Gaussian basis sets for use in correlated molecular calculations. I. The atoms boron through neon and hydrogen. *J. Chem. Phys.* **1989**, *90*, 1007−1023.
(38) Peterson, K. A.; Woon, D. E.; Dunning, T. H. Benchmark calculations with correlated molecular wave functions. IV. The classical barrier height of the H+H2→H2+H reaction. *J. Chem. Phys.* **1994**, *100*, 7410−7415.
(39) Schmidt, M. W.; Baldridge, K. K.; Boatz, J. A.; Elbert, S. T.; Gordon, M. S.; Jensen, J. H.; Koseki, S.; Matsunaga, N.; Nguyen, K. A.; Su, S.; et al. General atomic and molecular electronic structure system. *J. Comput. Chem.* **1993**, *14*, 1347−1363.
(40) Frisch, M. J.; Trucks, G. W.; Schlegel, H. B.; Scuseria, G. E.; Robb, M. A.; Cheeseman, J. R.; Scalmani, G.; Barone, V.; Mennucci, B.; Petersson, G. A.; Nakatsuji, H.; Caricato, M.; Li, H.; Hratchian, H. P.; Izmaylov, A. F.; Bloino, J.; Zheng, G.; Sonnenberg, J. L.; Hada, M.; Ehara, M.; Toyota, K.; Fukuda, R.; Hasegawa, J.; Ishida, M.; Nakajima, T.; Honda, Y.; Kitao, O.; Nakai, H.; Vreven, T.; Montgomery, J. A., Jr.; Peralta, J. E.; Ogliaro, F.; Bearpark, M. J.; Heyd, J. J.; Brothers, E. N.; Kudin, K. N.; Staroverov, V. N.; Kobayashi, R.; Normand, J.; Raghavachari, K.; Rendell, A.; Burant, J. C.; Iyengar, S. S.; Tomasi, J.; Cossi, M.; Rega, N.; Millam, J. M.; Klene, M.; Knox, J. E.; Cross, J. B.; Bakken, V.; Adamo, C.; Jaramillo, J.; Gomperts, R.; Stratmann, R. E.; Yazyev, O.; Austin, A. J.; Cammi, R.; Pomelli, C.; Ochterski, J. W.; Martin, R. L.; Morokuma, K.; Zakrzewski, V. G.; Voth, G. A.; Salvador, P.; Dannenberg, J. J.; Dapprich, S.; Daniels, A. D.; Farkas, O.; Foresman, J. B.; Ortiz, J. V.; Cioslowski, J.; Fox, D. J. *Gaussian 09*, revision D.01; Gaussian: Wallingford, CT, 2009.
(41) Barone, V. Anharmonic vibrational properties by a fully automated second-order perturbative approach. *J. Chem. Phys.* **2005**, *122*, 014108.
(42) Shimanouchi, T. *Tables of Molecular Vibrational Frequencies Consolidated, Volume I*; National Bureau of Standards: 1972; pp 1−160.
(43) Hunt, R. H.; Leacock, R. A.; Peters, C. W.; Hecht, K. T. Internal Rotation in Hydrogen Peroxide: The Far Infrared Spectrum and the Determination of the Hindering Potential. *J. Chem. Phys.* **1965**, *42*, 1931−1946.
(44) Camy-Peyret, C.; Flaud, J. M.; Johns, J. W. C.; Noël, M. Torsion-vibration interaction in H_2O_2: First high-resolution observation of $\nu 3$. *J. Mol. Spectrosc.* **1992**, *155*, 84−104.
(45) Bain, O.; Giguère, P. A. Hydrogen Peroxide and its Analogues: VI. Infrared Spectra of H_2O_2, D_2O_2, and HDO_2. *Can. J. Chem.* **1955**, *33*, 527−545.
(46) Giguére, P. A.; Srinivasan, T. K. K. A Raman study of H_2O_2 and D_2O_2 vapor. *J. Raman Spectrosc.* **1974**, *2*, 125−132.

DOI: 10.1021/acs.jctc.9b00665
J. Chem. Theory Comput. 2019, 15, 6840−6849

(47) Baumgärtel, H.; Jochims, H. W.; Rühl, E.; Bock, H.; Dammel, R.; Minkwitz, J.; Nass, R. *Inorg. Chem.* **1989**, *28*, 943−949.

DOI: 10.1021/acs.jctc.9b00665
J. Chem. Theory Comput. 2019, 15, 6840−6849